Nat Hazards (2009) 51:325–343
DOI 10.1007/s11069-008-9228-4

ORIGINAL PAPER

Tracking volcanic sulfur dioxide clouds for aviation hazard mitigation

Simon A. Carn · Arlin J. Krueger · Nickolay A. Krotkov · Kai Yang · Keith Evans

Received: 13 January 2008 / Accepted: 21 February 2008 / Published online: 20 March 2008

Abstract Satellite measurements of volcanic sulfur dioxide (SO_2) emissions can provide critical information for aviation hazard mitigation, particularly when ash detection techniques fail. Recent developments in space-based SO_2 monitoring are discussed, focusing on daily, global ultraviolet (UV) measurements by the Ozone Monitoring Instrument (OMI) on NASA's Aura satellite. OMI's high sensitivity to SO_2 permits long-range tracking of volcanic clouds in the upper troposphere and lower stratosphere (UTLS) and accurate mapping of their perimeters to facilitate avoidance. Examples from 2006 to 2007 include eruptions of Soufriere Hills (Montserrat), Rabaul (Papua New Guinea), Nyamuragira (DR Congo), and Jebel at Tair (Yemen). A tendency for some volcanic clouds to occupy the jet stream suggests an increased threat to aircraft that exploit this phenomenon. Synergy between NASA A-Train sensors such as OMI and the Atmospheric Infrared Sounder (AIRS) on the Aqua satellite can provide critical information on volcanic cloud altitude. OMI and AIRS SO_2 data products are being produced in near real-time for distribution to Volcanic Ash Advisory Centers (VAACs) via a NOAA website. Operational issues arising from these improved SO_2 measurements include the reliability of SO_2 as proxy for co-erupted ash, the duration of VAAC advisories for long-lived volcanic clouds, and the potential effects of elevated concentrations of SO_2 and sulfate aerosol in ash-poor clouds on aircraft and avionics (including cumulative effects after multiple inadvertent transits through dilute clouds). Further research is required in these areas. Aviation community assistance is sought through continued reporting of sulfurous odors or other indications of diffuse volcanic cloud encounters, in order to validate the satellite retrievals.

S. A. Carn (✉) · A. J. Krueger · K. Evans
Joint Center for Earth Systems Technology (JCET), University of Maryland
Baltimore County (UMBC), 1000 Hilltop Circle, Baltimore, MD 21250, USA
e-mail: scarn@umbc.edu

N. A. Krotkov · K. Yang
Goddard Earth Sciences and Technology (GEST) Center, UMBC, Baltimore, MD, USA

N. A. Krotkov · K. Yang
Laboratory for Atmospheres, Code 613.3, NASA Goddard Space Flight Center, Greenbelt, MD, USA

Keywords Sulfur dioxide · Volcanic clouds · Aviation hazards · Ultraviolet remote sensing

Abbreviations

AI	Aerosol Index
AIRS	Atmospheric Infrared Sounder
AVHRR	Advanced very high resolution radiometer
CALIOP	Cloud-Aerosol Lidar with Orthogonal Polarization
CALIPSO	Cloud-aerosol Lidar and Infrared Pathfinder Satellite Observation
CCD	Charge-coupled device
CNMI	Commonwealth of the Northern Mariana Islands
COSPEC	Correlation spectroscopy
DOAS	Differential optical absorption spectroscopy
EP	Earth Probe
EPA	Environmental Protection Agency
GOME	Global Ozone Monitoring Experiment
HYSPLIT	Hybrid Single-Particle Lagrangian Integrated Trajectory
IASI	Infrared Atmospheric Sounding Interferometer
IR	Infrared
LT	Local time
MLS	Microwave Limb Sounder
MODIS	Moderate Resolution Infrared Spectroradiometer
N7	Nimbus-7
NASA	National Aeronautics and Space Administration
NOAA	National Oceanic and Atmospheric Administration
NRT	Near real time
OMI	Ozone Monitoring Instrument
PBL	Planetary boundary layer
PNG	Papua New Guinea
SCIAMACHY	Scanning Imaging Absorption Spectrometer For Atmospheric Cartography
TES	Tropospheric Emission Spectrometer
TOMS	Total Ozone Mapping Spectrometer
UT	Universal time
UTLS	Upper troposphere and lower stratosphere
UV	Ultraviolet
VAAC	Volcanic Ash Advisory Center
VCD	Vertical column density
VEI	Volcanic Explosivity Index

1 Introduction

The synoptic perspective and global coverage of satellite imagery is crucial for effective mapping and tracking of volcanic eruption clouds for aviation hazard mitigation. Since the discovery in 1982 that ultraviolet (UV) Total Ozone Mapping Spectrometer (TOMS) data could be used to measure sulfur dioxide (SO_2) in volcanic clouds (Krueger 1983), observations of SO_2 have often been used to supplement operational volcanic ash

monitoring. The high sensitivity of UV measurements, particularly when SO_2 is injected into the upper troposphere/lower stratosphere (UTLS), along with typically low background SO_2 concentrations and its specificity to volcanic clouds (in the UTLS), results in a very low incidence of false detections, rendering them highly effective for this purpose. Three decades of TOMS measurements (Krueger et al. 1995, 2000; Carn et al. 2003; http://toms.umbc.edu) have shown that all major eruptions produce large amounts of SO_2, allowing volcanic clouds to be tracked long distances from their source.

Badly placed wavelengths and poor ground resolution (39–50 km at nadir) meant that TOMS measurements were restricted to the relatively high SO_2 amounts in large eruption clouds, although sensitivity was improved on the most recent model, Earth Probe (EP) TOMS. Consequently, the more frequent explosive eruptions of intermediate magnitude (with a Volcanic Explosivity Index (VEI) of 2–4; Newhall and Self 1982) were difficult to detect unless they were unusually sulfur-rich (e.g., the 1985 Nevado del Ruiz eruption; Krueger et al. 1990). Volcanic plumes generated by intermediate-scale eruptions have the potential to reach altitudes up to 25 km (Newhall and Self 1982), well within the stratosphere at all latitudes, and may occur several times a year, compared to roughly once per decade for events of VEI 5 or above (Simkin and Siebert 1994). Satellite-based detection of these frequent, smaller eruptions is thus essential for effective aviation hazard mitigation (Miller and Casadevall 2000).

Here we demonstrate the significant improvements in volcanic SO_2 detection and tracking ability offered by the latest generation of satellite sensors. We focus on instruments aboard spacecraft in NASA's A-Train ('Afternoon' Train; named thus due to the local afternoon overpass time) constellation, which consists of several polar-orbiting satellites flying in close formation. NASA's Aqua satellite (1:30 pm local time [LT] ascending node) leads the A-Train, followed by CloudSat (1:31 pm LT), Cloud-Aerosol Lidar and Infrared Pathfinder Satellite Observation (CALIPSO; 1:31 pm LT), the European PARASOL satellite (1:33 pm LT), and NASA's Aura satellite (1:38 pm LT). The result of this configuration is observation of the same air mass by multiple instrument suites within a 15-min time window, permitting studies of ephemeral phenomena such as clouds, and facilitating sensor inter-comparisons.

Several A-Train sensors can be used to detect and track volcanic emissions. Of particular note is the UV Ozone Monitoring Instrument (OMI), in orbit on the Aura platform since July 2004, which has unprecedented SO_2 sensitivity for a space-borne sensor. OMI is the latest of a new generation of charge-coupled device (CCD)-based hyperspectral UV/Visible spectrometers, building on the heritage of TOMS, and more recently the Global Ozone Monitoring Experiment (GOME; Burrows et al. 1999) and Scanning Imaging Absorption Spectrometer for Atmospheric Cartography (SCIAMACHY; Bovensmann et al. 1999). GOME and SCIAMACHY first demonstrated the advantages of high spectral resolution and full spectral coverage for space-based mapping of SO_2 and other trace gases in the lower troposphere and planetary boundary layer (PBL; Eisinger and Burrows 1998). OMI offers several improvements over these sensors, including better spatial resolution (13×24 km at nadir) and contiguous global coverage. As we demonstrate here, OMI's very high sensitivity to SO_2 and low noise permits long-range tracking of SO_2 clouds in the UTLS, detection of small volcanic eruptions, accurate mapping of volcanic cloud perimeters, and quantification of volcanic degassing in the lower troposphere and PBL.

The Atmospheric Infrared Sounder (AIRS) and Moderate Resolution Infrared Spectroradiometer (MODIS) on Aqua, and the Microwave Limb Sounder (MLS), and Tropospheric Emission Spectrometer (TES) on Aura, can also measure SO_2 of volcanic origin. Infrared (IR) AIRS, MODIS, and TES SO_2 retrievals using the 7.3 μm SO_2

absorption band are strongly dependent on the coincident water vapor column, with SO_2 measurements often restricted to the UTLS, particularly in the tropics (Carn et al. 2005; Prata et al. 2007). MLS detects microwave emission from the limb of the Earth's atmosphere and can measure volcanic SO_2 and HCl in the UTLS (e.g., Prata et al. 2007). CALIPSO, carrying the Cloud-Aerosol Lidar with Orthogonal Polarization (CALIOP), was launched in April 2006. CALIOP provides high-resolution vertical profiles of aerosol and clouds (with 60 m vertical resolution), and allows discrimination of cloud phase and detection of non-spherical aerosols (Winker et al. 2003).

In this article we begin by discussing the motivation for the use of SO_2 measurements (focusing on UV data) in aviation hazard mitigation. We then present some recent examples of eruptions detected by A-Train sensors, focusing on the application of OMI's high SO_2 sensitivity to long-range tracking of volcanic clouds. We also show how synergy among A-Train instruments can reveal key characteristics of volcanic clouds such as altitude, and document efforts to deliver pertinent data products to the aviation community in near real-time (NRT). Finally, we highlight some of the operational issues raised by the availability of these sensitive measurements.

2 The use of SO_2 measurements in aviation hazard mitigation: background and rationale

Rising volumes of jet aircraft traffic over the past three decades have lead to an increase in the number of aircraft flying in proximity to active volcanoes, numerous aircraft encounters with volcanic eruption clouds, and consequentially an increased awareness of volcanic ash hazards to aviation (Miller and Casadevall 2000). Airborne volcanic ash, comprised of fine-grained rock, mineral fragments, and glass shards generated during eruptions, is widely acknowledged to be the primary aviation hazard in drifting volcanic clouds. This material is capable of abrading forward-facing surfaces of aircraft, disrupting avionics and navigation systems, and impairing engine performance as it melts in the hot interior of jet engines and resolidifies in cooler sections. The consequences can range from minor superficial damage to airframes and reduction in visibility, to flame out and engine shutdown (Miller and Casadevall 2000).

Arguably the most hazardous volcanic clouds are those produced by explosive magmatic eruptions of silicic volcanoes. These involve hot, viscous magma that is disrupted explosively by high internal gas pressures as it ascends the volcanic conduit, producing hot, fine-grained ejecta that rises rapidly, powered initially by the vertical momentum of the gas-pyroclast mixture in the jet phase, and then by buoyant convection due to entrainment and heating of air by the hot ash in the convective phase (Carey and Bursik 2000). The thermal energy in explosive, magmatic eruption plumes allows them to quickly reach (and usually exceed) the cruising altitudes of jet aircraft (9–11 km). Since these eruptions are driven by magmatic gases, the resultant clouds are also gas-rich, with the dominant gases typically being water vapor (H_2O), carbon dioxide (CO_2), and SO_2 (SO_2 is the volatile sulfur species favored at the low pressures and high temperatures within an erupting volcano). Of these gases, SO_2 is by far the easiest to measure using remote sensing techniques. Although the ash and SO_2 may subsequently separate into distinct clouds under conditions of vertical wind shear as the ash falls out to lower altitudes (e.g., Schneider et al. 1999; Constantine et al. 2000), the presence of SO_2 is a robust indication that a magmatic eruption has occurred and that airborne ash is likely to be present.

Other eruption types can also be hazardous to aircraft under particular conditions. Small eruptions in tropical environments can be an aviation hazard, since in humid air eruption columns gain energy from latent heat of condensation of entrained water vapor, resulting in higher altitude plumes for a given mass eruption rate (Carey and Bursik 2000; Tupper et al. 2005). Effusive eruptions involve the discharge of large volumes of fluid basaltic magma, usually via gas-charged fire fountains along an eruptive fissure in their initial stages, followed by effusion of lava flows. The altitude attained by an effusive eruption plume depends on the mass eruption rate of magma, the fraction of hot ash produced by fragmentation, and the amount of heat transferred from the eruptive fountain to the air (Carey and Bursik 2000). Hence it is usually only the larger effusive eruptions involving extensive fissures that produce plumes hazardous to cruising aircraft: e.g., the 1984 Mauna Loa (Hawaii) eruption plume reached an altitude of 10–11 km (Smithsonian Institution 1984) and plumes generated by the larger eruptions of Nyamuragira (DR Congo) have reached altitudes of 10–15 km (Bluth and Carn 2008). Since the sulfur content of basalt is higher than more silicic magmas, effusive eruptions release large amounts of SO_2 that is easily detectable in UV satellite data (e.g., Bluth and Carn 2008). Generally, the amount of suspended ash in effusive eruption plumes is rapidly depleted downwind of the volcano due to coarser particle sizes relative to explosive eruption plumes. However, since the threshold concentration of ash that constitutes a threat to aircraft is currently unknown (Guffanti et al. 2005), such plumes must still be regarded as a potential aviation hazard (many airlines operate a zero tolerance policy with respect to volcanic ash; Cantor 1998).

Operational mitigation of the volcanic ash hazard is typically achieved by tracking airborne ash using satellite sensors with IR channels at 11 and 12 μm and the 'reverse absorption' or 'split-window' technique (Prata 1989a, b) or IR multispectral enhancements (e.g., Ellrod et al. 2003; Pavolonis et al. 2006). These algorithms exploit the inverse wavelength dependence of the imaginary refractive index of ash and water/ice in the 10–12 μm region of the IR. However, the techniques can fail to detect ash if the volcanic cloud is opaque (as in the early phase of many eruptions), if there is insufficient thermal contrast between the volcanic cloud and the underlying surface (e.g., if a cold volcanic cloud drifts over snow, ice, or high altitude meteorological clouds), or if the ash at higher altitudes is encased in ice (as is commonly observed in explosive eruption clouds; e.g., Rose et al. 1995). In fact, volcanic clouds are often tracked using the reverse absorption signal for ice rather than ash because of their high ice content (e.g., Tupper et al. 2007). The advantage of UV SO_2 (and ash) measurements is that they are relatively immune to these conditions. During the major eruption of Cerro Hudson (southern Chile) in August 1991, TOMS SO_2 and Aerosol Index (AI) measurements were more successful in tracking the volcanic clouds than IR advanced very high resolution radiometer (AVHRR) data due to the presence of subjacent cold meteorological clouds that hindered IR ash retrievals (Constantine et al. 2000).

The 1989–1990 eruption of Redoubt (Alaska) provided perhaps the earliest indication that even aged, dilute volcanic clouds are an aviation hazard. Two encounters with the December 15, 1989 volcanic cloud from Redoubt occurred on December 17 over western Texas, when the cloud was 35–55 h old and had drifted $\sim$5400 km from the volcano (Casadevall 1994). Elevated SO_2 was detected by N7-TOMS over Nevada and eastern California on December 16 and off the coast of Baja California on December 17 (Schnetzler et al. 1994). The December 17 encounters involved the loss of power to one engine on a Boeing 727 bound for El Paso, Texas, and minor leading edge abrasion on a US Navy DC-9 departing the El Paso area, both due to volcanic ash (Casadevall 1994). Since no volcanic ash was detected in the region at the time by satellite remote sensing, this

event demonstrated the utility of SO_2 measurements for long-range tracking of aged, but nevertheless hazardous, volcanic clouds. Although volcanic clouds from the next major Alaskan eruption, that of Mount Spurr in 1992, drifted over the conterminous United States and Canada (Bluth et al. 1995), no aircraft were damaged by encounters with the clouds due in part to effective use of satellite data, coupled with an increased awareness of volcanic cloud hazards after the Redoubt encounters (Casadevall and Krohn 1995).

The discussion above has focused on the use of SO_2 measurements as a proxy for ash, the primary aviation hazard. However, there is also evidence that SO_2 itself, and its oxidation product sulfuric acid (sulfate) aerosol, constitute an aviation hazard in their own right. During the sulfur-rich eruptions of El Chichón (Mexico) in 1982 and Pinatubo (Philippines) in 1991, large amounts of SO_2 were emplaced into the stratosphere, eventually converting to sulfate aerosol. For months or years after these eruptions, airlines reported an increase in the incidence of crazing of acrylic windows on jet aircraft, attributed to the effects of residual volcanogenic acid aerosol at cruising altitudes (Bernard and Rose 1990; Casadevall et al. 1996). Problems reported after the Pinatubo eruption included forward airframe damage, fading of polyurethane paint, and the accumulation of sulfate deposits (anhydrite and gypsum) in turbines, which blocked cooling holes and resulted in engine overheating (Casadevall et al. 1996). In June 1982, one year after the Pinatubo eruption, a jet suffered engine power loss caused by accumulated sulfate deposits, which were linked to the Pinatubo SO_2 emissions by isotopic analysis (Miller and Casadevall 2000).

Another potential hazard linked to volcanic SO_2 emissions is the haze and associated reduction of visibility due to scattering of light by sulfate aerosol, which is a concern at airports close to degassing volcanoes or in the path of drifting SO_2-rich clouds. During elevated activity at Anatahan volcano (CNMI) in 2005–2006, low-altitude haze impacted operations at the Andersen Air Force Base on Guam ($\sim$320 km from Anatahan) when winds carried the volcanic plume southward (C. R. Holliday, personal communication, 2005). The SO_2 cloud emitted by the 1984 Mauna Loa eruption created a drifting haze that reduced visibility to $\sim$3 km at the airport on Pohnpei (Micronesia), 5000 km from Hawaii, and also reached Guam, 6300 km distant (Smithsonian Institution 1984). Hence there is a clear case for SO_2 monitoring in its own right for aviation hazard mitigation, in addition to its use as a proxy for airborne volcanic ash.

3 The Ozone Monitoring Instrument (OMI)

OMI is a pushbroom sensor designed for daily, contiguous global mapping of ozone, SO_2 and several other trace gases with a nadir spatial resolution of 13 $\times$ 24 km (Levelt et al. 2006). For SO_2 measurements, the smaller footprint, higher spectral resolution (0.45 nm in the 306–380 nm UV2 channel), and full UV spectral coverage of OMI results in a two order of magnitude increase in sensitivity relative to TOMS, allowing detection of tropospheric volcanic plumes and small eruptions (Krotkov et al. 2006; Carn et al. 2008).

The SO_2 algorithm described by Krotkov et al. (2006) has been supplanted by an enhanced algorithm in the publicly released OMI SO_2 dataset (see http://so2.umbc.edu/omi), to improve the accuracy of retrievals for high SO_2 loadings. The new algorithm uses sets of discrete OMI wavelengths (up to 10) to simultaneously retrieve ozone, the SO_2 vertical column density (VCD) and the effective surface reflectivity (Yang et al. 2007). Six of the bands correspond to EP-TOMS wavelengths and four are centered at extrema of the SO_2 absorption cross-section in the 310.8–314.4 nm wavelength range. Longer wavelengths are

used for large SO_2 loadings to avoid underestimation of SO_2 due to saturation at shorter wavelengths. The algorithm requires a weighting function for SO_2, which is calculated based on assumed SO_2 profiles at prescribed altitudes. The default profile for SO_2 clouds in the UTLS is a vertical distribution between 15 and 20 km altitude, and for volcanic degassing in the free troposphere, we assume the SO_2 is distributed between 5 and 10 km altitude (Yang et al. 2007).

Between September 2004, when OMI began collecting data operationally, and December 2005, when the EP-TOMS mission ended, both OMI and EP-TOMS were operational, permitting comparisons between the validated TOMS SO_2 retrievals (Krueger et al. 1995, 2000) and OMI SO_2 data for volcanic eruptions. Figure 1 shows a comparison for the Manam (Papua New Guinea [PNG]) eruption of January 27, 2005. The volcanic cloud generated by this eruption reached an altitude of 21–24 km, and although ashfall from the cloud was reported, no split-window ash signal was detected in IR satellite imagery due to probable icing of ash particles (Tupper et al. 2007). However, TOMS and OMI measured high column amounts of SO_2 in the volcanic cloud (Fig. 1).

Although the TOMS and OMI retrievals are not coincident, the increased sensitivity, lower background noise and higher spatial resolution of the OMI retrieval are clear. The standard deviation of OMI SO_2 retrievals in SO_2-free background regions is 0.2–0.5 DU for clouds in the UTLS, while for TOMS SO_2 retrievals the range was 5–10 DU. This order of magnitude reduction in retrieval noise permits a more accurate delineation of the cloud perimeter in the OMI image, while the peak SO_2 column amounts in the core of the cloud are similar ($\sim$40–50 Dobson Units [DU]; 1 DU = 2.68×10^{16} molecules cm^{-2}), providing confidence in the OMI SO_2 measurements. Of particular note are the diffuse regions of SO_2 observed to the northeast and west of the main SO_2 cloud by OMI, which are largely lost in the noise in the TOMS image (Fig. 1), demonstrating the improved mapping of volcanic cloud hazards possible with OMI data.

4 Tracking volcanic clouds in the UTLS

OMI's high sensitivity ensures that most eruptions that produce SO_2 are detected regardless of magnitude, with the exception of high-latitude eruptions beyond the terminator. Nighttime eruptions cannot be detected in a timely manner by a UV instrument such as OMI, but residual SO_2 is typically detected on the following day for all but the smallest such events. The instrument is particularly effective for long-range tracking of SO_2 clouds in the UTLS. Several recent examples demonstrate this capability.

A lava dome collapse at Soufriere Hills volcano (SHV), Montserrat (West Indies), on May 20, 2006, triggered the release of a volcanic plume that entered the stratosphere (Carn et al. 2007; Prata et al. 2007). Shortly after the dome collapse, an ash cloud was reported at $\sim$17 km altitude by the Washington VAAC. Local atmospheric conditions were very calm on May 20, probably favoring the high altitude reached by the plume (Bursik 2001). OMI first detected the SO_2 cloud emitted from SHV at 17:00 UT on May 20, $\sim$6 h after emission, when it contained $\sim$0.2 Tg SO_2. The cloud then moved westward across the Caribbean Sea and the Pacific Ocean, at an average velocity of $\sim$13 m/s (Fig. 2). OMI continued to track the SO_2 cloud until June 13, when it became dispersed over a broad region from the Indian Ocean to Africa, at least 26,000 km from Montserrat. No ash was detected in the SO_2 cloud using the OMI UV AI, which is sensitive to absorbing aerosols. Coincident IR data also detected no significant amounts of ash (Prata et al. 2007), possibly due to icing of ash particles, although rapid fallout of dense ash is considered the most

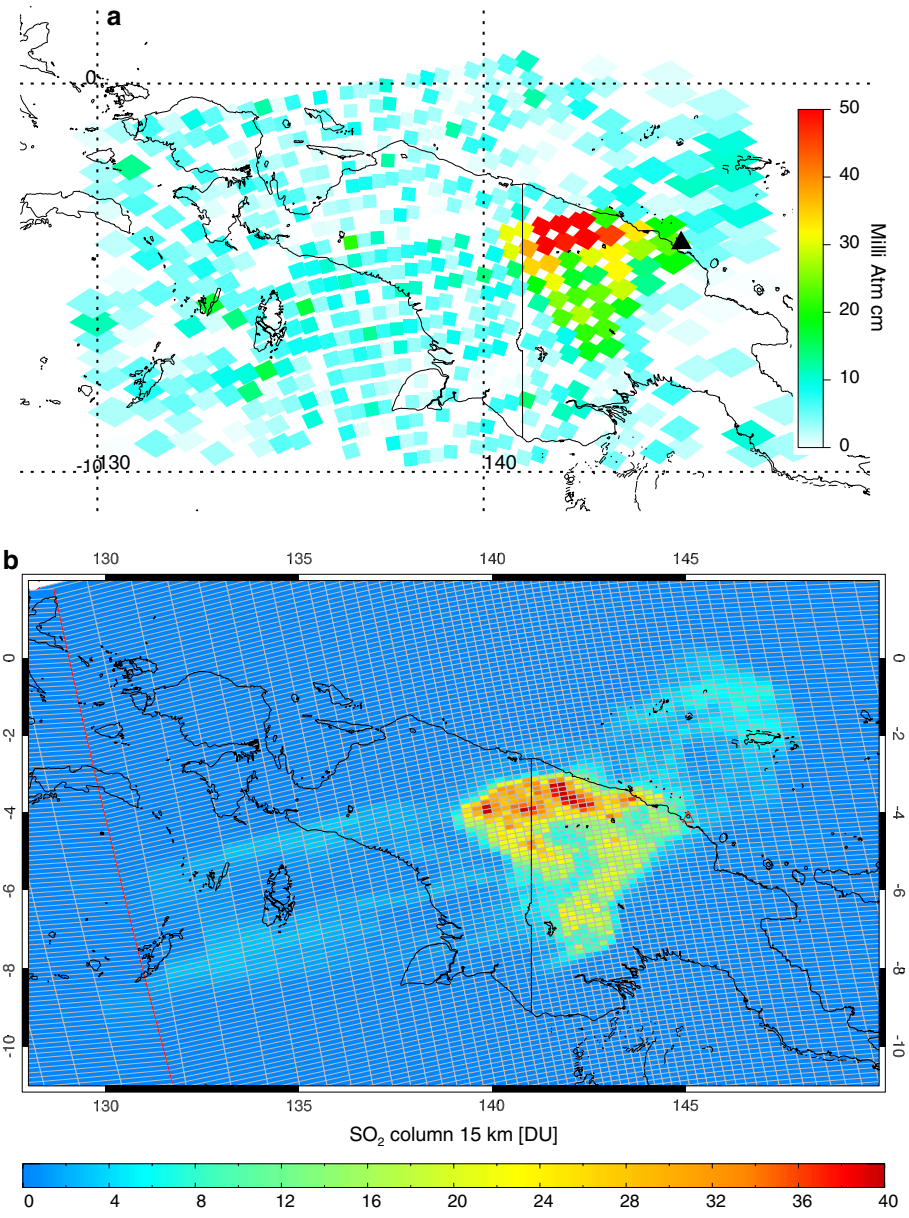

Fig. 1 Comparison of TOMS and OMI SO_2 retrievals for the Manam (Papua New Guinea) eruption of January 27, 2005 at 14:00 UT (00:00 LT on January 28). Both images show actual satellite footprints, which increase in size toward the edge of the orbit swath. (**a**) EP-TOMS overpass (orbit 45707) at 01:39–01:42 UT (11:39–11:42 LT) on January 28, 2005. *Color scale* shows retrieved SO_2 vertical column amount in milli atm cm (equivalent to Dobson Units). A *black triangle* indicates location of Manam; (**b**) OMI overpass (orbit 2867) at 04:13–04:15 UT (14:13–14:15 LT) on January 28. A *red triangle* indicates location of Manam; the *red line* to the left of the image is the edge of the next OMI orbit. Note the high background noise in the TOMS retrieval ($\sim$10 DU), which inhibits detection of the diffuse portions of the SO_2 cloud that can be seen northeast and west of the main cloud mass in the OMI image

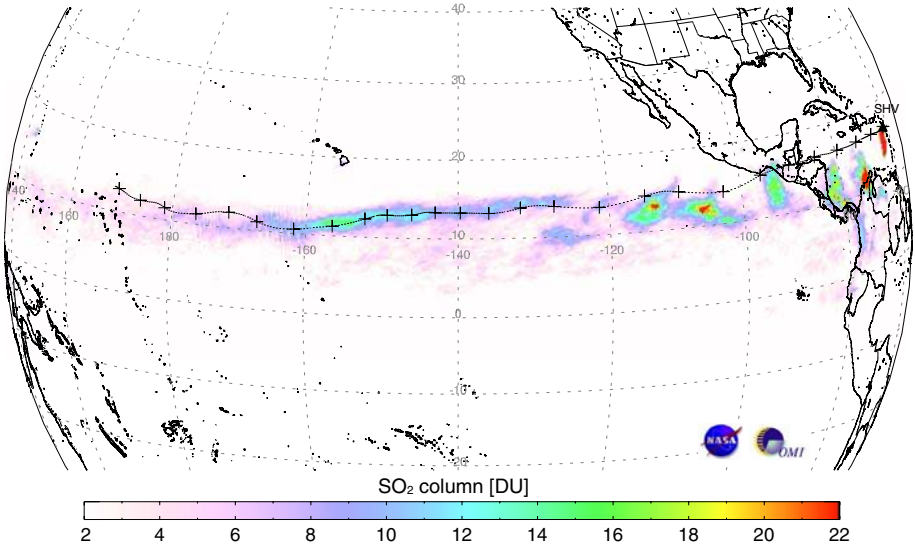

Fig. 2 Cumulative SO_2 VCDs measured by OMI in the SHV volcanic cloud from May 20 to June 6, 2006 as the cloud crossed the Pacific Ocean. The *dotted line* is a HYbrid Single-Particle Lagrangian Integrated Trajectory (HYSPLIT; Draxler and Rolph 2003; Rolph 2003) forward trajectory for a cloud at 20 km altitude, initialized at 11 UT on May 20 at SHV, with *crosses* plotted every 12 h. The trajectory covers 315 h (~13 days) of cloud transport

likely reason for the low ash content. This fact, combined with the cloud's high altitude (see below) above jet cruising levels, probably minimized the cloud's impact on aviation, with no aircraft encounters known to the authors.

With the exception of the first few days of atmospheric residence, the OMI SO_2 measurements fit a HYSPLIT trajectory for a cloud at 20 km altitude (Fig. 2). Confirmation of this altitude occurred when sulfate aerosol derived from the SO_2 was observed in backscatter data from the CALIOP lidar aboard CALIPSO in the A-Train. Fortuitously, CALIOP detected a scattering layer located at ~20 km altitude over the Philippines in its 'first-light' image collected on June 7, 2006 (Fig. 3; http://www.nasa.gov/mission_pages/calipso/news/First_Light.html). Inspection of the corresponding OMI SO_2 image confirmed that the layer comprised sulfate aerosol derived from the volcanic SO_2 (Fig. 3). CALIOP was still able to clearly detect the sulfate aerosol layer on 6 July (Fig. 3).

Another example of long-range SO_2 cloud transport occurred following the eruption of Rabaul (PNG) on October 7, 2006 (Fig. 4). The initial eruption cloud (with a reported altitude of 18 km) was ice-rich, similar to the 1994 Rabaul eruption (Rose et al. 1995), which impeded detection of high-level ash by IR sensors. OMI detected an SO_2 cloud containing ~0.23 Tg SO_2 at 02:30 UT on October 7. The cloud then split into two distinct parcels, one of which remained in the UTLS over PNG while the other rapidly traversed the southern Pacific (and South America) in the southern hemisphere jet stream (Fig. 4). Both clouds had dissipated below OMI detection limits by October 18. Due to the lower altitude of the Rabaul SO_2 cloud compared to the May 2006 SHV eruption, it was more difficult to locate in CALIPSO data (due to interference from meteorological clouds), but a sulfate aerosol signal was apparent east of PNG at an altitude of ~16 km on October 14, collocated with the coincident OMI SO_2 signal.

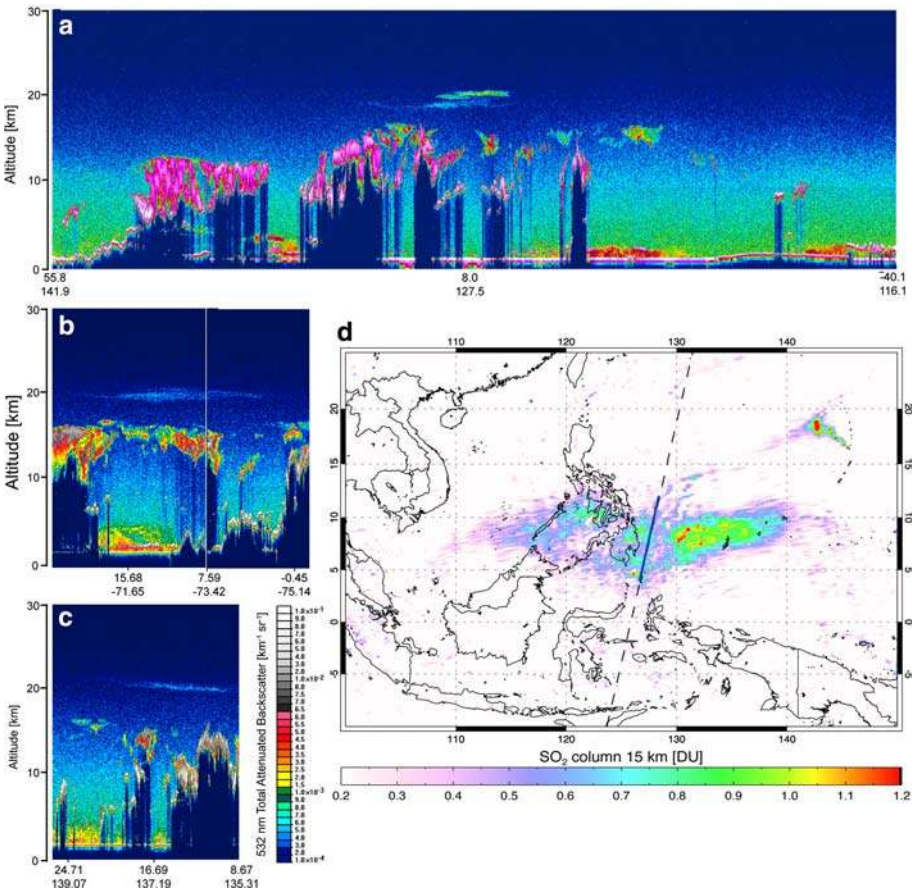

Fig. 3 CALIOP lidar curtains (532 nm attenuated backscatter) from the CALIPSO satellite, June 7–July 6, 2006. Latitudes and longitudes of locations along the CALIPSO ground-track are given below each image. (**a**) 'First-light' image on June 7, 2006 at 17:04 UT. The aerosol derived from the SHV SO_2 cloud is clearly seen as a scattering layer in the tropics at an altitude of ~20 km; (**b**) June 22 at 06:40 UT; (**c**) July 6 at 16:33 UT (adjacent color bar applies to all CALIOP images); (**d**) OMI SO_2 retrieval for the SHV volcanic cloud on June 7, 2006. The SO_2 from SHV is the coherent cloud at image center—note that a tropospheric SO_2 plume from Anatahan volcano (CNMI; 16.35° N, 145.67° E) is also visible. The *dashed line* shows the nighttime track of the CALIPSO spacecraft (approx. 12 h after Aura), with the *solid blue segment* indicating the approximate limits of the upper sulfate aerosol layer visible in (**a**). This conforms well to the margins of the SO_2 cloud mapped by OMI. All CALIOP data were taken under nighttime conditions. Depolarization measurements indicate that the aerosol in the layer was predominantly spherical, and therefore comprised mostly of sulfate aerosol

Two recent effusive eruptions that generated volcanic clouds at cruising altitudes occurred at Nyamuragira (DR Congo) in 2006 and Jebel at Tair (Yemen) in 2007 (Fig. 5). In the latter case, it was the first eruption of the volcano since 1883 and entirely unpredicted (Smithsonian Institution 2007). Both eruptions were largely effusive in nature but may have involved moderate explosive activity at their onset, particularly at Jebel at Tair. As Fig. 5 shows, OMI tracked the SO_2 clouds from these eruptions for at least two weeks, and trajectory modeling suggests maximum altitudes of ~10 km for both plumes. No volcanic ash was unambiguously detected in operational IR satellite imagery during either

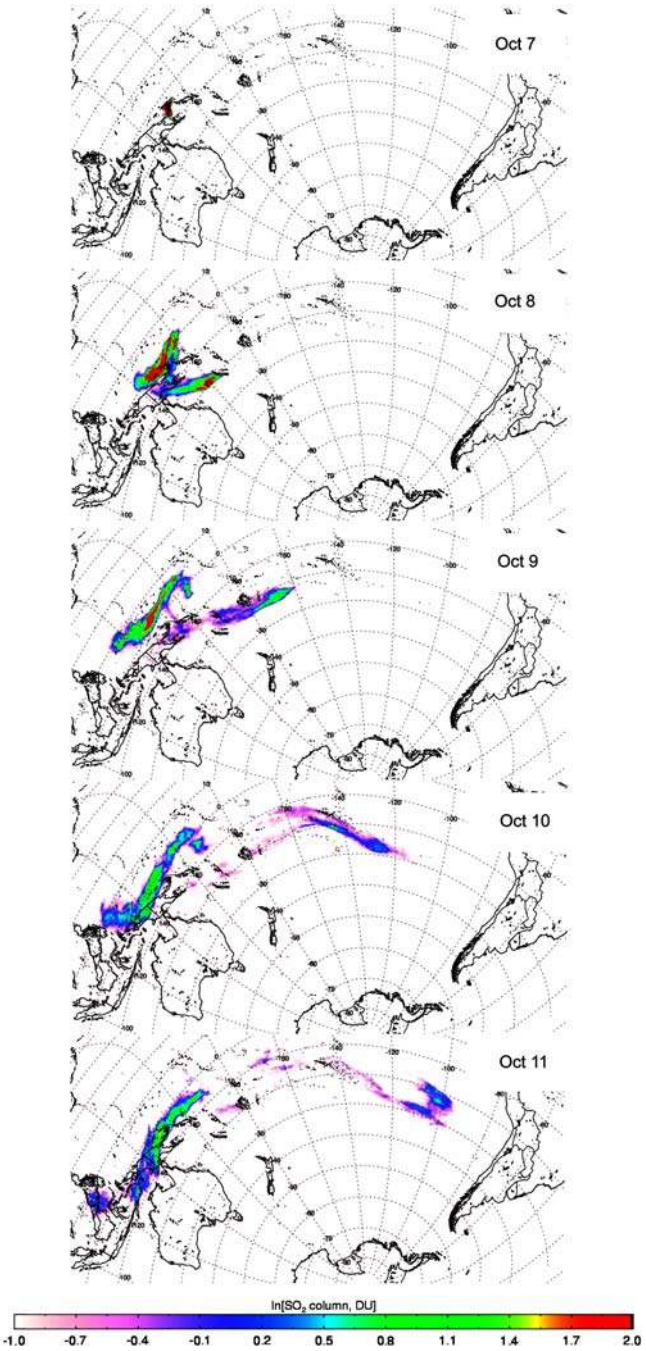

Fig. 4 Sequence of OMI SO_2 retrievals for the first 5 days of atmospheric residence of the Rabaul volcanic cloud in October 2006 (Oct 7–11). SO_2 VCDs are shown using a log scale

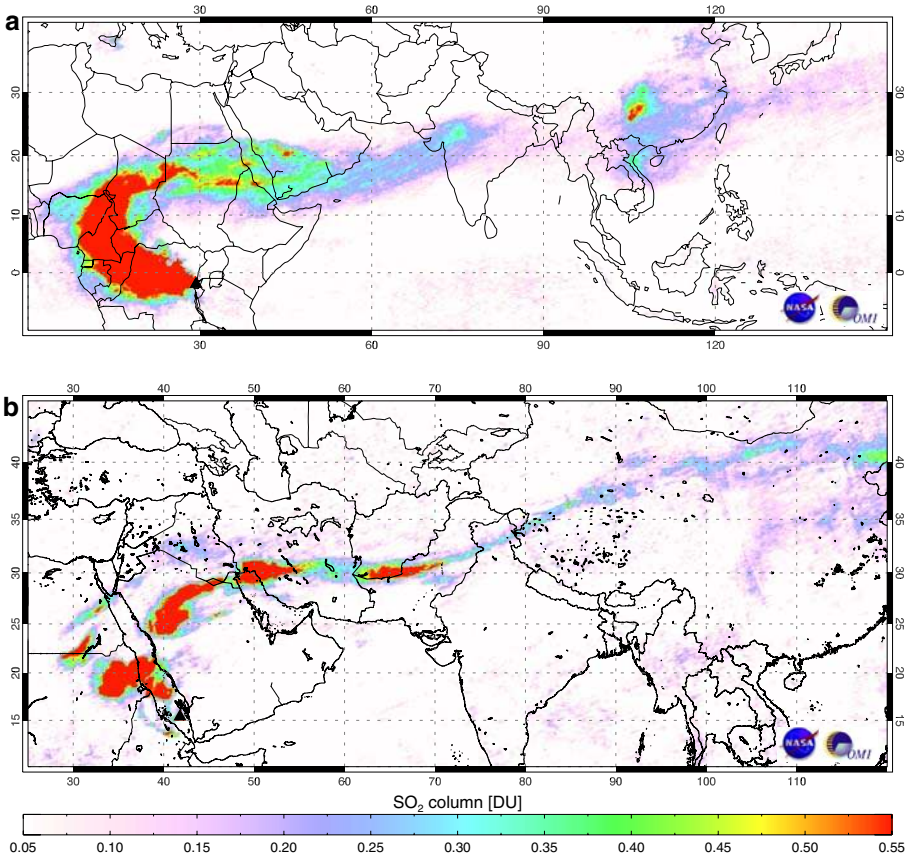

Fig. 5 OMI SO_2 maps for two volcanic clouds borne eastward by the subtropical jet stream. (**a**) SO_2 cloud produced by the eruption of Nyamuragira (DR Congo; 1.408° S, 29.2° E) that began on November 27, 2006. Average SO_2 VCDs retrieved from OMI data are shown for November 28–December 12, 2006, inclusive; (**b**) SO_2 cloud emitted by the eruption of Jebel at Tair (Yemen; 15.55° N, 41.82° E) that began on September 30, 2007. Average OMI SO_2 VCDs are shown for October 1–13, 2007, inclusive. The color scale is the same for both images. *Black triangles* indicate the locations of the volcanoes. In both images, some of the SO_2 measured over eastern China is due to anthropogenic pollution (e.g., the SO_2 feature at ~27° N, 105° E in (**a**))

eruption (water vapor interference was a major problem in the case of Nyamuragira). A KLM flight from Johannesburg to Amsterdam passing west of Nyamuragira on December 1 sighted the volcanic plume and diverted east of the volcano to avoid a potential encounter (G.J.A. Plaisier, written communication, 2006). As the SO_2 gained altitude downwind it encountered the subtropical jet stream and was carried eastward (Fig. 5a; this occurred from December 1 onward), suggesting that a diversion east of the volcano may not have guaranteed avoidance. However, inspection of daily OMI SO_2 maps indicates that the bulk of eastward transport of the plume did not occur until December 3.

Both the Nyamuragira and Jebel at Tair SO_2 clouds were borne eastward by the westerly subtropical jet stream upon reaching the altitude of this air current (Fig. 5). Movement of the Jebel at Tair cloud between consecutive OMI overpasses indicates that it traveled ~6000 km on October 5–6, 2007; an average speed of ~280 km/h. The significance of

this is that jet aircraft often exploit the high velocity jet stream winds on eastbound transcontinental routes to save time and fuel. In periods following volcanic eruptions that inject material to altitudes of ~10 km (or when drifting volcanic clouds reach this altitude), aircraft may therefore risk prolonged contact with volcanic gases and particles when occupying jet stream currents. This is a concern since even near-orthogonal, short duration encounters with dilute volcanic clouds (~10 min in the case of the February 2000 Hekla (Iceland) eruption cloud) have resulted in major damage to aircraft (Grindle and Burcham 2002; Rose et al. 2006).

Several examples discussed herein confirm that aircraft encounters with dilute and/or aged volcanic clouds are potentially damaging (e.g., Casadevall 1994; Grindle and Burcham 2002; Pieri et al. 2002). A more extreme case occurred on November 23–24, 2002, when two aircraft encountered ash and reported 'burn smells' at 10–11 km altitude to the northeast of PNG, resulting in damage to one of the aircraft (Tupper et al. 2006). Although trajectory analysis was inconclusive, Tupper et al. (2006) considered El Reventador (Ecuador), which had a major eruption into the UTLS on November 3–5, 2002, to be the most likely source, implying a cloud transit time across the Pacific Ocean of ~20 days. The sensitivity of EP-TOMS did not permit long-range tracking of dilute SO_2 clouds at the time. However, the total SO_2 mass emitted by the 2002 eruption of Reventador (~0.1 Tg) was of a similar order of magnitude to that produced by the SHV eruption in May 2006 (~0.2 Tg). Given that the SHV and Rabaul SO_2 clouds discussed above were tracked across the Pacific by OMI for 1–3 weeks, we surmise that the 2002 Reventador cloud would have been detected for at least 1–2 weeks, provided that it remained relatively coherent. This may have reduced the uncertainty regarding the origin of the volcanic cloud encountered over Micronesia.

5 Synergy of A-Train measurements and NRT data

We can use the OMI and CALIPSO data for the May 2006 SHV volcanic cloud to estimate local SO_2 concentrations that would have been experienced during an aircraft encounter. CALIPSO lidar profiles indicate a sulfate aerosol layer thickness of 1–2 km on June 7, 2006, when it was detected east of the Philippines over a distance of ~900 km (Fig. 3). OMI detected a maximum SO_2 VCD of ~1.2 DU in the cloud at this time, roughly equivalent to an SO_2 concentration of 0.08–0.16 ppm in a layer 1–2 km thick at 20 km altitude (assuming similar vertical distributions for SO_2 and aerosol). These amounts are below the levels at which SO_2 can generally be perceived by humans (0.3–1.4 ppm; IVHHN 2007), and the threshold concentration for perception of SO_2 is likely to be higher in the rarified atmosphere at cruising altitude.

As the altitude of the SHV cloud was well above cruising levels, in Fig. 6 we assume an altitude of 10 km and show SO_2 mixing ratio as a function of SO_2 VCD in a volcanic cloud of varying thickness. These crude estimates suggest that SO_2 would only be perceived in an aircraft in relatively fresh volcanic clouds (a few days old) containing more than ~10 DU of SO_2, depending on cloud thickness, which is often poorly constrained. Release of SO_2 from evaporation of sulfate aerosol in more aged clouds might increase the ambient SO_2 concentration, however. We note that ~0.5–1 ppmv SO_2 was measured during an inadvertent aircraft encounter with the February 2000 Hekla volcanic cloud at 10.4 km altitude when it was 33–34 h old (Rose et al. 2006) and contained ~30 DU of SO_2 (measured by EP-TOMS), but the cloud was only detected instrumentally and not by those onboard. Ambient air quality standards for SO_2 in the U.S. are 0.14 ppm and 0.5 ppm for 24 h and

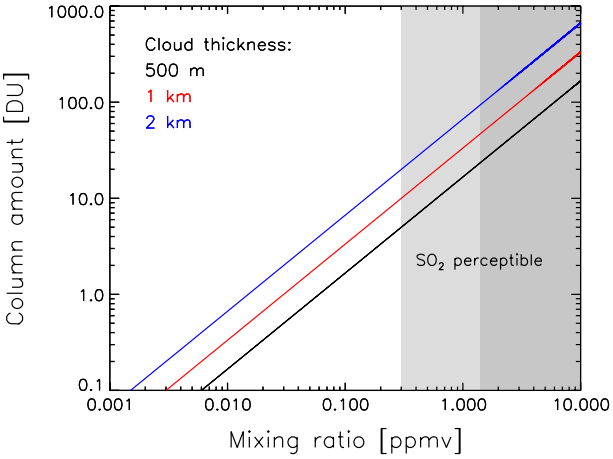

Fig. 6 Estimated SO_2 mixing ratios corresponding to measured VCDs in a volcanic cloud of variable thickness at 10 km altitude. SO_2 is usually perceptible by humans above ~0.3–1.4 ppm (IVHHN 2007)

3 h, respectively (not to be exceeded more than once per year; EPA 2007), which are unlikely to be exceeded unless prolonged contact with a drifting volcanic cloud occurs (e.g., in the jet stream).

Data from other A-Train sensors can also be utilized to reveal SO_2 cloud altitude. Since AIRS SO_2 retrievals are typically restricted to the UTLS (Prata and Bernardo 2007), whereas OMI provides a total column SO_2 measurement (in the absence of thick clouds), then calculating an OMI-AIRS residual SO_2 column (in daytime only) potentially provides information on the SO_2 vertical distribution. This is only possible because the Aura (OMI) and Aqua (AIRS) satellite overpasses occur within ~15 min of each other, minimizing any effects of cloud transport. Thus for a stratospheric SO_2 cloud, the OMI-AIRS residual column would be relatively small (providing the retrievals are correctly tuned for cloud altitude), whereas a lower tropospheric or PBL SO_2 cloud would produce a large residual.

We plan to exploit this synergy operationally in a system under development with NOAA (Vicente et al. 2007), using NRT OMI and AIRS SO_2 data to provide day and night coverage (CALIPSO data are currently not available in NRT). NRT data are available on the system within 3 h of the satellite overpass; while polar-orbiter data cannot match the timeliness of geostationary satellites they do offer significant advantages at high latitudes (e.g., the Kurile-Kamchatka-Aleutian arc in the north Pacific). In the future SO_2 data from the UV GOME−2 and the Infrared Atmospheric Sounding Interferometer (IASI) on the European MetOp-A platform (9:30 am LT descending node) will also be incorporated into the NRT system to supplement OMI and AIRS. GOME-2 and IASI have similar SO_2 sensitivity to OMI and AIRS, respectively. This will provide up to six SO_2 cloud images per day in NRT: GOME-2 and IASI at 9:30 am LT, AIRS at 1:30 pm LT, OMI at 1:45 pm LT, IASI at 9:30 pm LT, and AIRS at 1:30 am LT. Quantitative volcanic ash retrievals from OMI, AIRS, and other sensors will also be assimilated as ash algorithms are developed and refined, and an alert system for automated detection of large eruptions is also planned.

At the time of writing the NOAA NRT website is under development but operational (see http://gp16.ssd.nesdis.noaa.gov/pub/OMI/OMISO2/index.html). OMI orbits are posted to the website as they are received at NOAA, and composited on a global map. Subsets

are also available for volcanically active regions. Since the NRT OMI data are not archived (they use predicted ephemeris data to expedite processing), a companion website has been developed for the display of archived, science-quality OMI SO_2 data (http://so2.umbc.edu/omi). These data are typically produced a minimum of 12–24 h after the Aura overpass. Through the UMBC site interested parties can currently access daily OMI SO_2 maps for a collection of volcanically active regions dating back to May 2007, for retrospective visualization of volcanic degassing events (see below) and eruptions. For quantitative analysis, the complete OMI digital data archive is available at http://disc.sci.gsfc.nasa.gov/Aura/OMI/omso2.shtml.

6 Detection of tropospheric volcanic plumes

Increasing activity at many, if not all, volcanoes is manifested initially by increased gas emissions at the surface. SO_2 is released from rising high-temperature magma at shallow depths, and thus increased SO_2 degassing often presages magmatic eruptions. This has long been exploited in ground-based UV remote sensing using techniques such as correlation spectroscopy (COSPEC) and differential optical absorption spectroscopy (DOAS). However, satellite measurements of pre-eruptive degassing are challenging due to the low altitude of volcanic plumes (usually below 5 km) and the relatively small column amounts of SO_2 concerned.

GOME and SCIAMACHY first demonstrated that tropospheric SO_2 plumes from volcanoes could be measured using satellite data (Eisinger and Burrows 1998). OMI now offers similar sensitivity but with contiguous global coverage and better ground resolution. This is permitting the first daily measurements of passive volcanic degassing from space (e.g., Carn et al. 2008).

This new capability permits the collection of baseline SO_2 emission data for many infrequently monitored and/or remote volcanoes. As these data accrue it may be possible, through automated or operational monitoring of active or potentially active volcanoes, to recognize degassing trends that portend magmatic eruptions (in conjunction with other geophysical datasets) and provide advance warning to the aviation community. Furthermore, in tropical regions subject to strong convection, monitoring of tropospheric emissions (both from passive degassing and small explosive eruptions) is necessary to assess possible lofting of volcanic material emitted at lower altitudes to higher altitudes within convection cells, which can be enhanced by the input of volcanic heat (e.g., Tupper et al. 2005). However, significant further research (observations and modeling) on the degassing patterns expected prior to explosive eruptions is needed to enable exploitation of tropospheric SO_2 measurements for aviation hazard mitigation. Further algorithm development and validation studies are also needed to improve the accuracy of lower tropospheric SO_2 retrievals, particularly in the PBL, to permit confident recognition of day-to-day variations in SO_2 emissions.

7 Discussion

The increased fidelity and sensitivity of SO_2 measurements from OMI and similar sensors facilitates volcanic cloud mapping and long-range tracking, and will provide many opportunities for trajectory model validation. However, the detection of much lower SO_2 concentrations in volcanic clouds also raises several operational issues. These include the

degree to which SO_2 is a reliable indicator of the spatial extent of co-erupted ash, the duration of VAAC advisories for volcanic clouds with long atmospheric residence times, and the potential effects of elevated concentrations of SO_2, sulfate aerosol and other acid gases in ash-poor clouds on aircraft and avionics (including cumulative effects after multiple inadvertent and unnoticed transits through dilute clouds). Regarding the latter point, and given the numerous aircraft encounters with dilute volcanic clouds that have caused damage, routine monitoring of the location (and altitude) of volcanic SO_2 clouds could potentially assist airlines in an assessment of long-term, cumulative exposure to airborne volcanic gases and aerosols, particularly in aircraft that frequent volcanically active regions.

Most of the questions above cannot be properly addressed without further research. However, there seems to be little doubt that operational SO_2 monitoring by VAACs would substantially reduce the incidence of 'undetected' volcanic clouds. It is well known that SO_2 and ash components in volcanic clouds can separate, and may travel in different directions depending on wind shear (e.g., Schneider et al. 1999). Hence monitoring of both ash and SO_2 is necessary to obtain a complete picture of the aviation hazard. Use of SO_2 data can be crucial for effective tracking of ice-rich volcanic clouds where icing of ash particles inhibits their explicit detection (e.g., Tupper et al. 2007).

While ingestion of ash into jet engines is certainly more damaging than ingestion of SO_2 and other acid gases or aerosols, further work on the potential effects of SO_2, other acid gases and acid aerosol on airframes and avionics (and also on flight crew and passengers) is urgently needed. Reports of engine flameouts after encounters with apparently dilute volcanic clouds (e.g., Tupper et al. 2006) underscore this need. Some potentially relevant work has been done on the effects of SO_2 on fuel oxidation (Alzueta et al. 2001), which may have implications for the behavior of a jet engine (particularly the combustion chamber) during a volcanic cloud encounter. The potential effects of the exotic chemical environment of volcanic clouds on jet engine performance warrant further research. Recognition by the aviation community of the potential significance of sulfurous odors detected during flight (e.g., IAVWOPSG 2005) is an important step toward elucidating the hazard due to dilute volcanic clouds, and the incidence of aircraft encounters with them. Reporting of sulfur gases encountered at altitude, and inspection of coincident satellite data from instruments such as OMI, will permit a rigorous evaluation of the strengths and limitations of current space-borne SO_2 measurements when applied to improving aviation hazard warnings.

8 Summary

Numerous examples demonstrate the ability of OMI, CALIPSO, and other A-Train sensors to track volcanic clouds from a range of eruption magnitudes for extended periods, promising improved mitigation of volcanic cloud hazards to aviation. OMI's high sensitivity to SO_2 provides a new tool to investigate long-range transport of volcanic clouds, validate trajectory models, detect small eruptions, and monitor pre-eruptive SO_2 degassing from volcanoes. Rapid observation by multiple A-Train instrument suites permits measurement of volcanic aerosol altitude and inter-comparison of satellite retrievals. The observation that several recent eruptions have injected volcanic gases into the subtropical jet stream suggests increased vulnerability and exposure to hazardous conditions in aircraft that exploit these currents. A-Train data will be supplemented by observations from the European MetOp satellites in a NRT operational system to detect and track volcanic SO_2

clouds. A future challenge is to combine these multiple, advanced satellite measurements (plus ground-based observations at active volcanoes) into an effective aviation hazard warning system.

Acknowledgments Funding for this work was provided by the NASA Science Mission Directorate's Earth-Sun System Division. The OMI project is managed by Royal Dutch Meteorological Institute (KNMI) and the Netherlands Agency for Aerospace Programs (NIVR). The NOAA Air Resources Laboratory (ARL) is acknowledged for provision of the HYSPLIT model and READY website (http://www.arl.noaa.gov/ready.html) used in this work.

References

Alzueta MU, Bilbao R, Glarborg P (2001) Inhibition and sensitization of fuel oxidation by SO_2. Combust Flame 127:2234–2251

Bernard A, Rose WI (1990) The injection of sulfuric acid aerosols in the stratosphere by the El Chichón volcano and its related hazards to the international air traffic. Nat Hazards 3:59–67

Bluth GJS, Carn SA (2008) Exceptional sulfur degassing from Nyamuragira volcano, 1979–2005. Int J Remote Sens (in press)

Bluth GJS, Scott CJ, Sprod IE, Schnetzler CC, Krueger AJ, Walter LS (1995) Explosive emissions of sulfur dioxide from the 1992 Crater Peak eruptions, Mount Spurr volcano, Alaska. In: Keith TEC (ed) The 1992 eruptions of Crater Peak vent, Mount Spurr volcano, Alaska. U.S. Geological Survey Bulletin 2139, pp 37–45

Bovensmann H, Burrows JP, Buchwitz M, Frerick J, Noël S, Rozanov VV, Chance KV, Goede AHP (1999) SCIAMACHY—Mission objectives and measurement modes. J Atmos Sci 56(2):127–150

Burrows JP, Weber M, Buchwitz M, Rozanov V, Ladstätter-Weissenmayer A, Richter A, de Beek R, Hoogen R, Bramstedt K, Eichmann K-U, Eisinger M, Perner D (1999) The Global Ozone Monitoring Experiment (GOME): Mission concept and first scientific results. J Atmos Sci 56:151–175

Bursik M (2001) Effect of wind on the rise height of volcanic plumes. Geophys Res Lett 28(18):3621–3624

Cantor R (1998) Complete avoidance of volcanic ash is only procedure that guarantees flight safety. ICAO Mag 53(18–19):26

Carey S, Bursik M (2000) Volcanic plumes. In: Sigurdsson H (ed) Encyclopedia of volcanoes. Academic Press, San Diego, CA, pp 527–544

Carn SA, Krueger AJ, Bluth GJS, Schaefer SJ, Krotkov NA, Watson IM, Datta S (2003) Volcanic eruption detection by the Total Ozone Mapping Spectrometer (TOMS) instruments: a 22-year record of sulfur dioxide and ash emissions, In: Oppenheimer C, Pyle DM, Barclay J (eds) Volcanic degassing. Geological Society, London, Special Publications, 213, pp 177–202

Carn SA, Strow LL, de Souza-Machado S, Edmonds Y, Hannon S (2005) Quantifying tropospheric volcanic emissions with AIRS: the 2002 eruption of Mt. Etna (Italy). Geophys Res Lett 32, L02301, doi: 10.1029/2004GL021034

Carn SA, Krotkov NA, Yang K, Hoff RM, Prata AJ, Krueger AJ, Loughlin SC, Levelt PF (2007) Extended observations of volcanic SO_2 and sulfate aerosol in the stratosphere. Atmos Chem, Phys Discuss 7:2857–2871 [Available online from http://www.atmos-chem-phys-discuss.net/7/2857/2007/acpd-7-2857-2007.html]

Carn SA, Krueger AJ, Krotkov NA, Arellano S, Yang K (2008) Daily monitoring of Ecuadorian volcanic degassing from space. J Volcanol Geotherm Res (in press)

Casadevall TJ (1994) The 1989–90 eruption of Redoubt volcano, Alaska: impacts on aircraft operations. J Volcanol Geotherm Res 62:301–316

Casadevall TJ, Krohn MD (1995) Effects of the 1992 Crater Peak eruptions on airports and aviation operations in the United States and Canada. In: Keith TEC (ed) The 1992 eruptions of Crater Peak vent, Mount Spurr volcano, Alaska. U.S. Geological Survey Bulletin 2139, pp 205–220

Casadevall TJ, Delos Reyes PJ, Schneider DJ (1996) The 1991 Pinatubo eruptions and their effects on aircraft operations. In: Newhall CG, Punongbayan RS (eds) Fire and mud: eruptions and lahars of Mount Pinatubo, Philippines. University of Washington Press, Seattle/London, pp 1071–1088

Constantine EK, Bluth GJS, Rose WI (2000) TOMS and AVHRR observations of drifting volcanic clouds from the August 1991 eruptions of Cerro Hudson. In: Mouginis-Mark PJ, Crisp JA, Fink JH (eds) Remote sensing of active volcanism. Geophysical monograph 116, American Geophysical Union, Washington, DC, pp 45–64

Draxler RR, Rolph GD (2003) HYSPLIT (HYbrid Single-Particle Lagrangian Integrated Trajectory) Model, access via NOAA ARL READY Website (http://www.arl.noaa.gov/ready/hysplit4.html). NOAA Air Resources Laboratory, Silver Spring, MD

Eisinger M, Burrows JP (1998) Tropospheric sulfur dioxide observed by the ERS-2 GOME instrument. Geophys Res Lett 25:4177–4180

Ellrod GP, Connell BH, Hillger DW (2003) Improved detection of airborne volcanic ash using multispectral infrared satellite data. J Geophys Res 108:4356, doi:10.1029/2002JD002802

EPA (2007) National Ambient Air Quality Standards (NAAQS). [Available online from http://epa.gov/air/criteria.html]

Grindle TJ, Burcham FW Jr (2002) Even minor ash encounters can cause major damage to aircraft. ICAO J 57:12–30

Guffanti M, Ewert JW, Gallina GM, Bluth GJS, Swanson GL (2005) Volcanic-ash hazard to aviation during the 2003–2004 eruptive activity of Anatahan volcano, Commonwealth of the Northern Mariana Islands. J Volcanol Geotherm Res 146:241–255

IAVWOPSG (2005) Further evaluation of including smell of sulfur as a reportable element in the AIREP. International Airways Volcano Watch Operations Group, Working Paper IAVWOPSG/2-WP/32. [Available at: http://www.icao.int/anb/iavwopsg/meetings/iavwopsg2/wp/WP32.pdf]

IVHHN (2007) Gas and aerosol guidelines for sulfur dioxide (SO_2) [Available at: http://www.esc.cam.ac.uk/ivhhn/guidelines/gas/so2.html]

Krotkov NA, Carn SA, Krueger AJ, Bhartia PK, Yang K (2006) Band residual difference algorithm for retrieval of SO_2 from the Aura Ozone Monitoring Instrument (OMI). IEEE Trans Geosci Remote Sens 44(5):1259–1266, doi:10.1109/TGRS.2005.861932

Krueger AJ (1983) Sighting of El Chichon sulfur dioxide clouds with the Nimbus 7 total ozone mapping spectrometer. Science 220:1377–1379

Krueger AJ, Walter LS, Schnetzler CC, Doiron SD (1990) TOMS measurement of the sulfur dioxide emitted during the 1985 Nevado del Ruiz eruptions. J Volcanol Geotherm Res 41:7–15

Krueger AJ, Walter LS, Bhartia PK, Schnetzler CC, Krotkov NA, Sprod I, Bluth GJS (1995) Volcanic sulfur dioxide measurements from the total ozone mapping spectrometer instruments. J Geophys Res 100:14057–14076

Krueger AJ, Schaefer S, Krotkov N, Bluth G, Barker S (2000) Ultraviolet remote sensing of volcanic emissions. In: Mouginis-Mark PJ, Crisp JA, Fink JH (eds) Remote sensing of active volcanism. Geophysical Monograph 116, American Geophysical Union, Washington, DC, pp 25–43

Levelt PF, van den Oord GHJ, Dobber MR, Mälkki A, Visser H, De Vries J, Stammes P, Lundell JOV, Saari H (2006) The ozone monitoring instrument. IEEE Trans Geosci Remote Sens 44(5):1093–1101, doi:10.1109/TGRS.2006.872333

Miller TP, Casadevall TJ (2000) Volcanic ash hazards to aviation. In: Sigurdsson H (ed) Encyclopedia of volcanoes. Academic Press, San Diego, CA, pp 915–930

Newhall CG, Self S (1982) The volcanic explosivity index (VEI): an estimate of explosive magnitude for historical volcanism. J Geophys Res 87:1231–1238

Pavolonis MJ, Feltz WF, Heidinger AK, Gallina GM (2006) A daytime complement to the reverse absorption technique for improved automated detection of volcanic ash. J Atmos Ocean Tech 23:1422–1444

Pieri D, Ma C, Simpson JJ, Hufford G, Grindle T, Grove C (2002) Analyses of in-situ airborne volcanic ash from the February 2000 eruption of Hekla volcano, Iceland. Geophys Res Lett 29(16):1767, doi:10.1029/2001GL013688

Prata AJ: 1989a, Observations of volcanic ash clouds in the 10–12-micron window using AVHRR/2 data. Int J Remote Sens 10:751–761

Prata AJ: 1989b, Radiative transfer calculations for volcanic ash clouds. Geophys Res Lett 16:1293–1296

Prata AJ, Bernardo C (2007) Retrieval of volcanic SO_2 column abundance from Atmospheric Infrared Sounder data. J Geophys Res 112, D20204, doi:10.1029/2006JD007955

Prata AJ, Carn SA, Stohl A, Kerkmann J (2007) Long range transport and fate of a stratospheric volcanic cloud from Soufrière Hills volcano, Montserrat. Atmos Chem Phys 7:5093–5103 (http://www.atmos-chem-phys.net/7/5093/2007/acp-7-5093-2007.html)

Rolph GD (2003) Real-time Environmental Applications and Display system (READY) Website [http://www.arl.noaa.gov/ready/hysplit4.html], NOAA Air Resources Laboratory, Silver Spring, MD

Rose WI, Delene DJ, Schneider DJ, Bluth GJS, Krueger AJ, Sprod I, McKee C, Davies HL, Ernst GGJ (1995) Ice in the 1994 Rabaul eruption cloud: implications for volcano hazard and atmospheric effects. Nature 375:477–479

Rose WI, Millard GA, Mather TA, Hunton DE, Anderson B, Oppenheimer C, Thornton BF, Gerlach TM, Viggiano AA, Kondo Y, Miller TM, Ballenthin JO (2006) Atmospheric chemistry of a 33–34 hour old

volcanic cloud from Hekla Volcano (Iceland): insights from direct sampling and the application of chemical box modeling. J Geophys Res 111, D20206, doi:10.1029/2005JD006872
Schneider DJ, Rose WI, Coke LR, Bluth GJS, Sprod I, Krueger AJ (1999) Early evolution of a stratospheric volcanic eruption cloud as observed with TOMS and AVHRR. J Geophys Res 104(D4):4037–4050
Schnetzler CC, Doiron SD, Walter LS, Krueger AJ (1994) Satellite measurement of sulfur dioxide from the Redoubt eruptions of 1989–1990. J Volcanol Geotherm Res 62:353–357
Simkin T, Siebert L (1994) Volcanoes of the world, 2nd edn. Geoscience Press, Tucson, AZ
Smithsonian Institution (1984) Mauna Loa, Scientific Event Alert Network (SEAN) 9(4) (http://www.volcano.si.edu/world/volcano.cfm?vnum=1302-02=&volpage=var#sean_0903)
Smithsonian Institution (2007) Jebel at Tair, Bulletin of the Global Volcanism Network 32(10) (http://www.volcano.si.edu/world/volcano.cfm?vnum=0201-01=&volpage=var#bgvn_3210)
Tupper A, Oswalt JS, Rosenfeld D (2005) Satellite and radar analysis of the volcanic-cumulonimbi at Mount Pinatubo, Philippines, 1991. J Geophys Res 110, doi:10.1029/2004JD005499
Tupper A, Davey J, Stewart P, Stunder B, Servranckx R, Prata F (2006) Aircraft encounters with volcanic clouds over Micronesia, Oceania, 2002–03. Aust Met Mag 55:289–299
Tupper A, Itikarai I, Richards M, Prata AJ, Carn SA, Rosenfeld D (2007) Facing the challenges of the International Airways Volcano Watch: the 2004/05 eruptions of Manam, Papua New Guinea. Weather Forecast 22(1):175–191
Vicente G, Serafino G, Krueger A, Carn S, Yang K, Krotkov N, Guffanti M, Levelt P (2007) The NOAA near real-time OMI-SO_2 cloud visualization and product distribution system. EOS Trans AGU 88(52), Fall Meet Suppl, Abstract V31A-0293
Winker DM, Pelon J, McCormick MP (2003) The CALIPSO mission: Spaceborne lidar for observation of aerosols and clouds. Proc SPIE 4893:1–11
Yang K, Krotkov NA, Krueger AJ, Carn SA, Bhartia PK, Levelt PF (2007) Retrieval of large volcanic SO_2 columns from the Aura Ozone Monitoring Instrument: comparison and limitations. J Geophys Res 112, D24S43, doi:10.1029/2007JD008825